JACS
JOURNAL OF THE AMERICAN CHEMICAL SOCIETY

Communication

pubs.acs.org/JACS

Nanoreactors for Studying Single Nanoparticle Coarsening

Jinan Chai,[†,‡] Xing Liao,[‡,§] Louise R. Giam,[‡,§] and Chad A. Mirkin*[,†,‡,§]

[†]Department of Chemistry, [‡]International Institute for Nanotechnology, and [§]Department of Materials Science and Engineering, Northwestern University, 2145 Sheridan Road, Evanston, Illinois 60208, United States

Supporting Information

ABSTRACT: The ability to observe intermediate structures as part of coarsening processes that lead to the formation of single nanoparticles (NPs) is important in gaining fundamental insight pertaining to nanostructure growth. Here, we use scanning probe block copolymer lithography (SPBCL) to create "nanoreactors" having attoliter volumes, which confine Au NP nucleation and growth to features having diameters <150 nm on a substrate. With this technique, one can use in situ TEM to directly observe and study NP coarsening and differentiate Ostwald ripening from coalescence processes. Importantly, the number of metal atoms that can engage in coarsening can be controlled with this technique, and TEM "snapshots" of particle growth can be taken. The size of the resulting nanostructures can be controlled in the 2−10 nm regime.

The distinct optical, electrical, and catalytic properties of nanoparticles (NPs) have made them a focus of nanoscience research since they have promising applications spanning the fields of photonics, electronics, catalysis, and biological sensors.[1−3] Fundamental chemistry and materials science issues concerning the physical and chemical properties of NPs are directly related to their morphology and dimensions, as dictated by their growth processes. Such synthetic goals require mechanistic understandings of NP nucleation and coarsening; current approaches for studying these phenomena typically rely on sampling bulk solutions at multiple time points as representative snapshots of what is occurring.[4−6] Though observations of nanostructure evolution in TEM are possible with specialty liquid chambers, the dynamics of NP changes happen in nanoliter volumes that are relatively large compared to the size of individual particles.[7] Herein, we describe a novel way to directly study the intermediates that lead to single NP formation within site-specifically positioned attoliter "nanoreactors" defined by scanning probe block copolymer lithography (SPBCL). SPBCL is a recently developed method that allows one to deliver and position small volumes of metal-coordinated block copolymers on a surface for the controlled synthesis of individual NPs.[8] Importantly, this approach provides a unique way to dictate the resulting NP dimensions by (1) defining the concentration of the metal precursor within the polymer nanoreactors and (2) delivering certain volumes of block copolymers to a substrate. We rationalize that, by controlling the energetics of the system (e.g., temperature), SPBCL could be used to visualize coarsening at the single Au NP level. Thus, while studying the site-specific synthesis of such single Au NPs by SPBCL, we have directly observed in situ coarsening processes resulting in the formation of single sub-10 nm NPs within a block copolymer feature in the TEM.

SPBCL relies on scanning probe-based methods such as dip-pen nanolithography (DPN)[9−13] or polymer pen lithography (PPL)[14−16] to deliver attoliter volumes of block copolymers coordinated to metal ions in a parallel manner over large areas. The block copolymer acts as a synthetic "nanoreactor" and confines NP precursor ions on a substrate. Once the block copolymer−metal ion ink has been patterned, plasma treatment is used to reduce the metal ions and remove the polymer, leaving behind a single NP within each patterned feature. NP dimensions are dictated by the block copolymer feature size, which can be controlled by adjusting the tip−substrate contact time or amount of force applied to the polymer pens in the case of PPL. In a typical SPBCL experiment, chloroauric acid ($HAuCl_4$) is added to an aqueous solution of poly(ethylene oxide)-block-poly(2-vinylpyridine) (PEO-*b*-P2VP). After stirring for 24 h, the metal ion-coordinated block copolymer mixture was coated onto scanning probes, which were then used for lithography. The block copolymer precursor spots are deposited, and subsequent removal of the organic polymer and reduction of the metal ions result in the formation of single NPs within the original patterned locations (Figure 1a). The Au NPs in the array are monodisperse and, in this experiment, have an average diameter of 8.5 ± 0.5 nm. High-resolution TEM (HRTEM) shows that each Au NP is a face-centered-cubic (fcc) single crystal where the (111) interplanar spacing is 2.4 Å (Figure 1b). The fast Fourier transform (FFT) of the HRTEM image also confirms the single crystal nature of the Au NPs.

An important aspect of SPBCL is that the synthesized Au NP has dimensions that are not only smaller than the original block copolymer feature size, but also an atomic force microscope (AFM) tip radius (~10 nm). In previous work, it has been shown that the Au NPs have sizes about one tenth of the original patterned feature volume (the volume of this feature controls the number of atoms).[8] Based on this trend, one would need to pattern a 50 nm block copolymer feature (with a height of ~15 nm) to form a 5 nm Au NP. Routinely generating block copolymer features that are 50 nm or smaller, however, remains challenging because of AFM tip radius limitations and the water meniscus that forms between the tip and substrate. Moreover, polymer pens used in a PPL experiment typically have diameters of ~70 nm,[14,15] which makes it even more difficult to pattern a 50 nm block copolymer feature. Therefore, another strategy needs to be

Received: October 25, 2011
Published: December 13, 2011

   dx.doi.org/10.1021/ja2097964 | *J. Am. Chem.Soc.* 2012, 134, 158−161

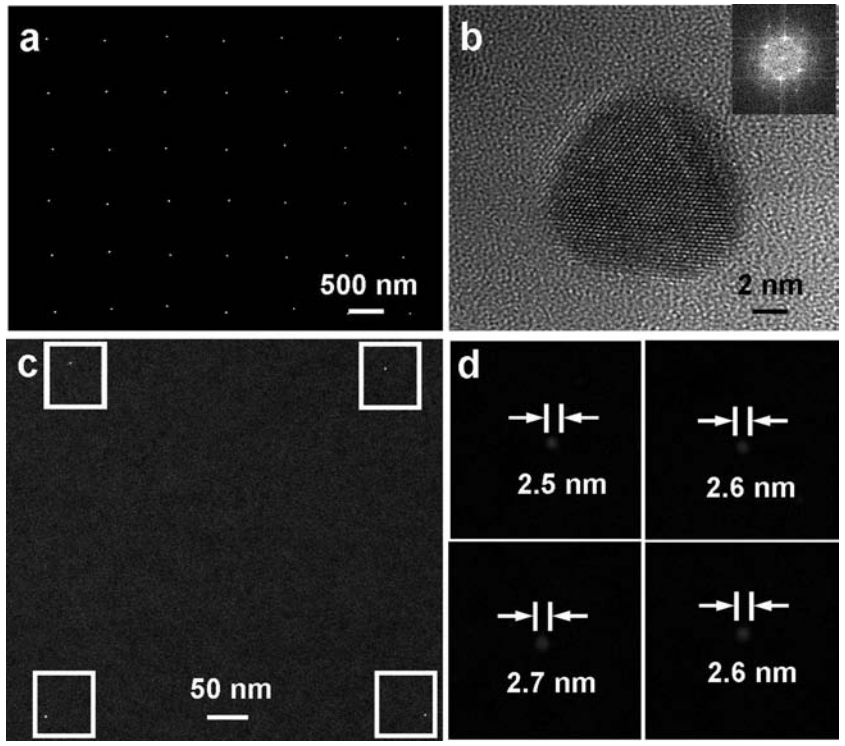

Figure 1. (a) TEM image of an array of Au NPs with diameters of 8.5 ± 0.5 nm synthesized by SPBCL. (b) HRTEM image of a Au NP generated by SPBCL; FFT of the HRTEM image shows its single crystal structure (inset). (c) TEM image of an array of four sub-3 nm gold NPs made by SPBCL. (d) A higher magnification view of each of the four NPs in (c).

developed to obtain sub-5 nm NPs. As the nitrogen of the pyridine units in the P2VP block coordinates to metal ions such as Au^{3+},[17,18] the molar ratio of gold ions to 2-vinylpyridine (2VP) determines the local concentration of ions within the block copolymer feature; for block copolymer features of the same size, ones with a lower gold concentration should result in smaller Au NPs. For example, when the molar ratio of gold to 2VP is reduced to 1:4 in the block copolymer ink, sub-5 nm single crystal Au NPs form. Furthermore, when the molar ratio of gold to 2VP is reduced to 1:8 and the original feature of block copolymer ink is ∼90 nm in diameter, a single sub-3 nm NP within each patterned feature is generated (Figure 1c and 1d).

Though it is not possible to directly observe the formation of single Au NPs during plasma treatment, we have observed that the high energy electron beam in a TEM can also induce the formation of single particles. Using this approach and in situ TEM, one can use SPBCL-generated features to study NP coarsening processes such as Ostwald ripening and coalescence.[19,20] We used a TEM having a cooled cryo-sample holder to increase the time between coarsening events and enable observations of nanostructure intermediates leading up to the single particle end result.

Time and temperature are two factors that dictate the dynamics of coarsening.[21] Temperature affects metal ion and nanocluster diffusion coefficients; dynamic coarsening processes, which would be too fast to distinguish at room temperature, are decelerated when the temperature is decreased. At lower temperatures, one can observe the intermediate states that lead to single particle formation. Time-lapse images of coarsening events leading to the synthesis of an ∼10 nm Au NP (1:2 molar ratio of Au to 2VP) within a block copolymer spot were obtained beginning at −30 °C with increments of 10 °C over 3 min (Gatan cryostage, after focusing the electron beam). When images were first taken, there was already a large Au NP and a number of small Au nanocrystals inside the block copolymer feature (faint halo) from nucleation under electron beam radiation (Figure 2a). When the substrate temperature increased, the number of particles decreased significantly, and eventually at room temperature, there is only one particle, analogous to the structures observed after plasma treatment (Figure 1). At −120 °C, the coarsening process becomes even slower, which enables us to investigate the process in detail. TEM images (Figure 2b) show that, under isothermal conditions, a large number of Au nanocrystals (diameters ranging from 1 to 2 nm) emerge around the 10 nm Au NP during the initial nucleation process. Images taken in series as a function of time reveal that the particles remained immobile during the experiment, while the size of the surrounding small particles gradually decreased and eventually disappeared. In another experiment, when we magnify the area around an 8 nm Au NP, instead of the small Au nanocrystals decreasing in size, they can be seen as moving toward and finally merging with the big 8 nm NP (Figure 2c and Supporting Information Movie S1).

Figure 3 shows a sequence of TEM images for a block copolymer solution having a 1:4 molar ratio of Au to 2VP that leads to the synthesis of a sub-5 nm Au NP upon continuous electron beam irradiation at −120 °C. A large number of ultrasmall Au nanocrystals can be seen in the first few images. Different from the previous case, Au nanocrystals migrate toward neighboring nanocrystals and subsequently coalesce into larger clusters. The process continues until one single NP is obtained. The most notable consequence of this coarsening process is the simultaneous decrease in the number of particles and increase in the average particle size. When the molar ratio

dx.doi.org/10.1021/ja2097964 | J. Am. Chem.Soc. 2012, 134, 158−161

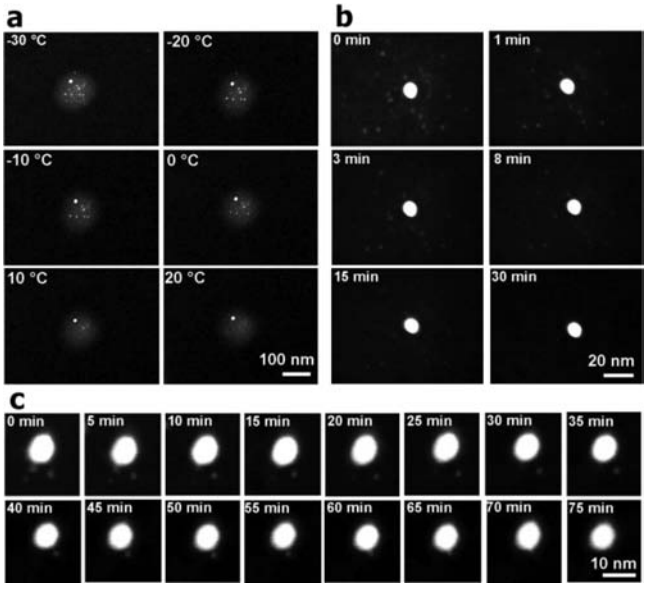

Figure 2. In situ TEM observation of Au NP coarsening in SPBCL-defined block copolymer features. The molar ratio of gold to 2VP is 1:2. (a) The number of particles decreases with increasing substrate temperature from −30, −20, −10, 0, 10, to 20 °C. The time interval between images is ∼200 s. (b) Small particles gradually disappear via ripening at −120 °C. (c) Three small particles coalesce into the adjacent big NP at −120 °C.

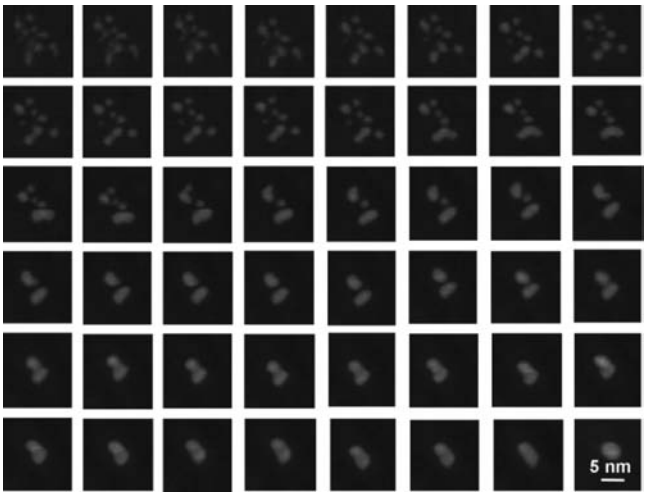

Figure 3. Time-lapse TEM images taken at −120 °C which reveal the growth trajectory of a sub-5 nm Au NP within the same SPBCL-defined spot upon continuous electron beam irradiation. The molar ratio of gold to 2VP is 1:4. Note that coarsening occurs here via migration and coalescence. The time interval between images is ∼1 min.

of gold to 2VP is 1:8, fewer nanocrystals are nucleated after electron beam exposure as compared with the higher gold concentrations (cryo-sample holder is at −120 °C). In one particular block copolymer feature, only three Au NPs (∼1 nm in diameter, with interparticle spacing of ∼1.5 nm) were observed after electron beam irradiation (Figure 4, first image). NP coarsening can be seen in the subsequent images with a time interval of ∼1 min where the two particles in the upper right (1 and 2) first migrate toward and then coalesce with each other. Then this particle (1*) merges with the bottom left particle (3) to form a slightly elongated particle. This particle

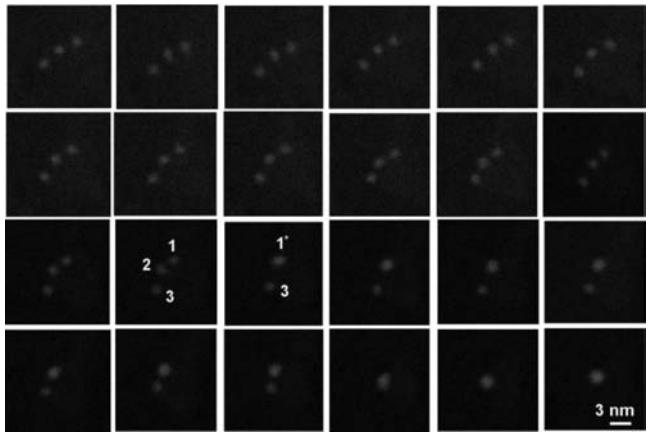

Figure 4. A series of TEM images taken at −120 °C illustrating the dynamic aggregation and coalescence of three 1 nm Au NPs into one 2.6 nm Au NP. The molar ratio of gold to 2VP is 1:8. The time interval between images is ∼1 min.

then gradually restructures into a nearly spherical particle with a diameter of 2.6 nm. During this process, the motion of particles can be clearly distinguished from random migration and Ostwald ripening.

The coarsening of small nanoclusters can be governed by Ostwald ripening or coalescence. In Ostwald ripening, surface atoms of small particles have larger free energies and therefore increased probabilities of diffusing to larger particles. During Ostwald ripening, the size of smaller particles decreases and the size of larger particles increases even though each particle's center of mass rarely moves (Figure 2b). Ostwald ripening, however, cannot solely explain the movement of particles observed in Figures 2c, 3, and 4, which implies that, in certain cases for SPBCL, coalescence also facilitates Au NP coarsening. Indeed, literature references indicate that two particles may coalesce for Au NP systems.[22] The driving force for the coalescence of two particles may be from surface energy reduction where the new NP surface area is less than that of the sum of the original particle surface areas.[23] In particular, in situ TEM observations also suggest that the coalescence of NPs resulted from the direct migration of small particles toward the large one. A possible explanation for the attractive migration of these particles may be attributed to differences in atomic diffusion along the particle edges that is driven by nonuniform chemical potentials around the particle.[24] When the molar ratio of Au to 2VP is 1:2, we have observed that both Ostwald ripening (Figure 2a, b) and coalescence (Figure 2c) can occur. Why one coarsening mechanism dominates over another can likely be attributed to interparticle separation. It has been reported that coalescence can occur for pairs of similarly sized particles separated by distances less than ∼4.5r (where r is the particle radius).[24] Consistent with literature, small particles having diameters between 1 and 2 nm (Figure 2c) that are no more than ∼5 nm from the large particle edge were observed to undergo coalescence. Moreover, when the block copolymer feature is large (>100 nm in diameter, Figure 2a) and at higher Au concentrations (Au to 2VP is 1:2, Figure 2b), multiple nanocrystal nucleation events can occur with large interparticle separation distances. Though these distances preclude coalescence, Ostwald ripening can still take place. In contrast, when the block copolymer feature is small and at lower Au concentrations (Figures 3, 4), not only do fewer nanocrystals nucleate, but they also have smaller interparticle separation

dx.doi.org/10.1021/ja2097964 | J. Am. Chem.Soc. 2012, 134, 158−161

distances, which can lead to direct migration and coalescence. It is important to note that, for these discussed conditions, though one mechanism (Ostwald ripening or coalescence) may appear dominant, both processes are likely to be occurring concomitantly.

In summary, we have developed a method based upon SPBCL and in situ TEM to observe the dynamics of Au NP coarsening for particles as small as 2 nm. This approach allows one to confine a set number of Au^{3+} ions within positionally defined block copolymer "nanoreactors" having attoliter volumes to limit the reaction environment and directly monitor site-specific NP coarsening. Indeed, the ability to visualize and separate Ostwald ripening from particle coalescence processes which lead to the synthesis of single NPs can be useful for understanding the more general mechanisms of nanostructure formation. Such NP formation work could ultimately yield insight on and address fundamental questions in catalysis, chemical synthesis, interfacial phenomena, and nanoparticle synthesis beyond noble metal structures.[25]

■ ASSOCIATED CONTENT

Supporting Information

Movies of nanoparticle coarsening. This material is available free of charge via the Internet at http://pubs.acs.org.

■ AUTHOR INFORMATION

Corresponding Author

chadnano@northwestern.edu

■ ACKNOWLEDGMENTS

C.A.M. acknowledges the U.S. Air Force Office of Scientific Research (AFOSR), the Defense Advanced Research Projects Agency (DARPA), and NSF (NSEC program) for support of this research. J.C. acknowledges the Natural Sciences and Engineering Research Council of Canada (NSERC) for a Postdoctoral Fellowship. L.R.G. acknowledges an ARCS scholarship. The authors thank the Northwestern University Electron Probe Instrumentation Center for help with TEM.

■ REFERENCES

(1) Klein, D. L.; Roth, R.; Lim, A. K. L.; Alivisatos, A. P.; McEuen, P. L. *Nature* **1997**, *389*, 699.
(2) Bakr, O. M.; Amendola, V.; Aikens, C. M.; Wenseleers, W.; Li, R.; Dal Negro, L.; Schatz, G. C.; Stellacci, F. *Angew. Chem., Int. Ed.* **2009**, *48*, 5921.
(3) Graham, D.; Faulds, K.; Smith, W. E. *Chem. Commun.* **2006**, 4363.
(4) Kim, B. J.; Tersoff, J.; Kodambaka, S.; Reuter, M. C.; Stach, E. A.; Ross, F. M. *Science* **2008**, *322*, 1070.
(5) Meli, L.; Green, P. F. *ACS Nano* **2008**, *2*, 1305.
(6) Ruffino, F.; Grimaldi, M. G.; Giannazzo, F.; Roccaforte, F.; Raineri, V.; Bongiorno, C.; Spinella, C. *J. Phys. D: Appl. Phys.* **2009**, 42.
(7) Zheng, H. M.; Smith, R. K.; Jun, Y. W.; Kisielowski, C.; Dahmen, U.; Alivisatos, A. P. *Science* **2009**, *324*, 1309.
(8) Chai, J. A.; Huo, F. W.; Zheng, Z. J.; Giam, L. R.; Shim, W.; Mirkin, C. A. *Proc. Natl. Acad. Sci. U.S.A.* **2010**, *107*, 20202.
(9) Piner, R. D.; Zhu, J.; Xu, F.; Hong, S. H.; Mirkin, C. A. *Science* **1999**, *283*, 661.
(10) Piner, R. D.; Mirkin, C. A. *Langmuir* **1997**, *13*, 6864.
(11) Ginger, D. S.; Zhang, H.; Mirkin, C. A. *Angew. Chem., Int. Ed.* **2004**, *43*, 30.
(12) Zhou, X. Z.; Boey, F.; Huo, F. W.; Huang, L.; Zhang, H. *Small* **2011**, *7*, 2273.
(13) Zhou, X. Z.; Boey, F.; Zhang, H. *Chem. Soc. Rev.* **2011**, *40*, 5221.
(14) Huo, F. W.; Zheng, Z. J.; Zheng, G. F.; Giam, L. R.; Zhang, H.; Mirkin, C. A. *Science* **2008**, *321*, 1658.
(15) Liao, X.; Braunschweig, A. B.; Zheng, Z. J.; Mirkin, C. A. *Small* **2010**, *6*, 1082.
(16) Giam, L. R.; Mirkin, C. A. *Angew. Chem., Int. Ed.* **2011**, *50*, 7482.
(17) Chai, J.; Wang, D.; Fan, X. N.; Buriak, J. M. *Nat. Nanotechnol.* **2007**, *2*, 500.
(18) Spatz, J. P.; Sheiko, S.; Moller, M. *Macromolecules* **1996**, *29*, 3220.
(19) Baldan, A. *J. Mater. Sci.* **2002**, *37*, 2171.
(20) Birtcher, R. C.; Donnelly, S. E.; Song, M.; Furuya, K.; Mitsuishi, K.; Allen, C. W. *Phys. Rev. Lett.* **1999**, *83*, 1617.
(21) Arcidiacono, S.; Bieri, N. R.; Poulikakos, D.; Grigoropoulos, C. P. *Int. J. Multiphase Flow* **2004**, *30*, 979.
(22) Chen, Y.; Palmer, R. E.; Wilcoxon, J. P. *Langmuir* **2006**, *22*, 2851.
(23) Lewis, L. J.; Jensen, P.; Barrat, J. L. *Phys. Rev. B* **1997**, *56*, 2248.
(24) Yang, W. C.; Zeman, M.; Ade, H.; Nemanich, R. J. *Phys. Rev. Lett.* **2003**, *90*, 136102.
(25) Liu, X.; Fu, L.; Hong, S.; Dravid, V. P.; Mirkin, C. A. *Adv. Mater.* **2002**, *14*, 231.